

Tritium β decay in pionless EFT

Jared Vanasse

Ohio University

June 30, 2017

Recipe for EFT($\not{\pi}$)

- ▶ For momenta $p < m_\pi$ pions can be integrated out as degrees of freedom and only nucleons and external currents are left.
- ▶ Write down all possible terms of nucleons and external currents that respect symmetries (rotational, isospin).
- ▶ Develop a power counting to organize terms by their relative importance.
 - ▶ Organized by counting powers of momentum.
 - ▶ Ensure order-by-order results are renormalization group invariant (converge to finite values for $\Lambda \rightarrow \infty$).
 - ▶ Check that various sets of observables converge as expected.
- ▶ Calculate respective observables up to a given order in the power counting.

Two- and Three-Body Inputs of EFT(π)

Two-body inputs for EFT(π):

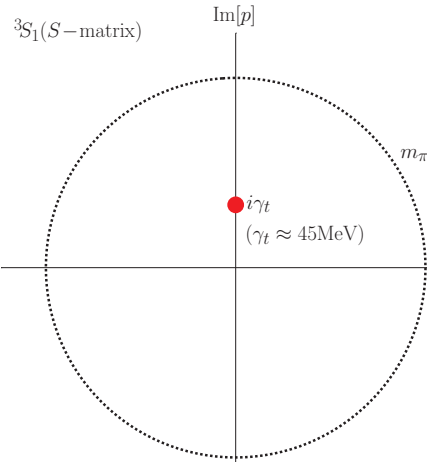
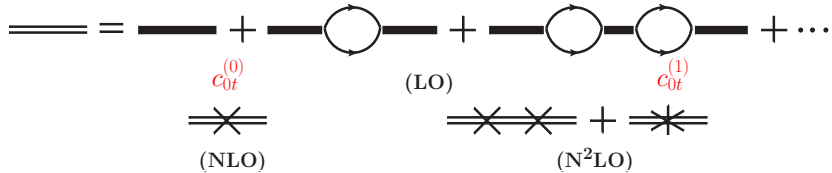
- ▶ LO scattering lengths in a_1 (3S_1) and a_0 (1S_0) **non-perturbative**
- ▶ NLO range corrections r_1 and r_0 **perturbative**
- ▶ N²LO SD-mixing term **perturbative**

Three-body inputs for EFT(π):

- ▶ LO three-body force H_0 fit to doublet S -wave nd scattering length **non-perturbative** ([Bedaque et al.](#)) nucl-th/9906032
- ▶ NNLO three-body energy dependent three-body force H_2 fit to triton binding energy **perturbative**

Total of **6** NNLO parameters, ignoring SD-mixing.

The LO dressed deuteron propagator is given by a bubble sum



(Z-parametrization) At LO coefficients are fit to reproduce the deuteron pole and at NLO to reproduce the residue about the deuteron pole (Phillips et al. (2000)) nucl-th/9908054.

LO Triton Vertex function

Triton vertex function given by infinite sum of diagrams at LO

$$\begin{aligned} \text{Diagram A} &= \text{Diagram B} + \text{Diagram C} + \text{Diagram D} + \dots \\ \text{Diagram E} &= \text{Diagram F} + \text{Diagram G} + \text{Diagram H} + \dots \end{aligned}$$

The diagrams consist of three horizontal lines meeting at a central red circle. In the first row (Diagram A), the top line has two solid lines and one dashed line. In the second row (Diagram E), the top line has one solid line and two dashed lines. Diagrams B, C, D, F, G, and H are variations where the lines are rearranged or include additional internal lines.

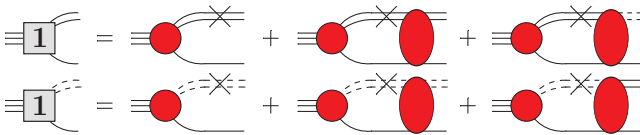
Infinite sum is represented by integral equation that is solved numerically

$$\begin{aligned} \text{Diagram A} &= \text{Diagram B} + \text{Diagram C} + \text{Diagram D} + \dots \\ \text{Diagram E} &= \text{Diagram F} + \text{Diagram G} + \text{Diagram H} + \dots \end{aligned}$$

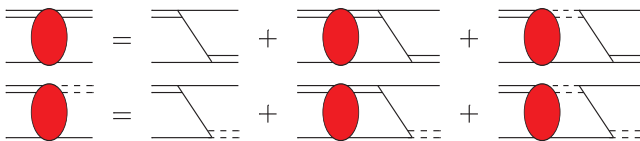
The diagrams are identical to those in the previous row, showing the same set of vertex functions and their decomposition into a sum of loop corrections.

NLO Triton Vertex function

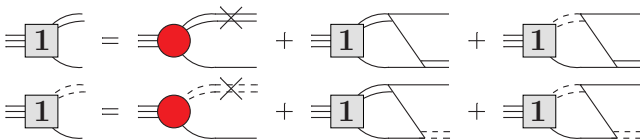
NLO triton vertex function given by sum of diagrams



where

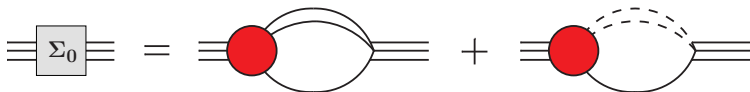


Can also be solved by set of integral equations



LO Three-Nucleon Propagator

Defining



The dressed three-nucleon propagator is given by the sum of diagrams



which yields

$$\begin{aligned} i\Delta_3(E) &= \frac{i}{\Omega} - \frac{i}{\Omega} H_{\text{LO}} \Sigma_0(E) \frac{i}{\Omega} + \dots \\ &= \frac{i}{\Omega} \frac{1}{1 - H_{\text{LO}} \Sigma_0(E)}, \end{aligned}$$

Higher-Order Three-Nucleon Propagator

Defining the functions

$$\Sigma_1 = \text{Diagram 1} + \text{Diagram 2}$$
$$\Sigma_2 = \text{Diagram 3} + \text{Diagram 4}$$

The NNLO three-nucleon propagator is

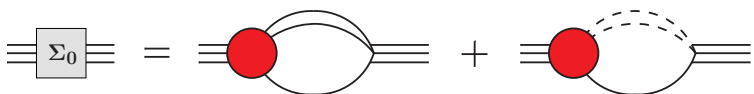
$$\begin{aligned} & \text{Diagram } \Sigma_1 + H_{\text{NLO}} \text{Diagram } \Sigma_0 \\ & (\text{NLO}) \\ & \text{Diagram } \Sigma_2 + H_{\text{NLO}} \text{Diagram } \Sigma_1 + H_{\text{NNLO}} \text{Diagram } \Sigma_0 \\ & + \text{Diagram } \Sigma_1 \text{Diagram } \Sigma_1 + 2H_{\text{NLO}} \text{Diagram } \Sigma_0 \text{Diagram } \Sigma_1 \\ & + (H_{\text{NLO}})^2 \text{Diagram } \Sigma_0 \text{Diagram } \Sigma_0 + \text{Diagram } h_2 \\ & (\text{NNLO}) \end{aligned}$$

Properly Renormalized Vertex Function

- ▶ Three-body forces are fit to ensure triton propagator has pole at triton binding energy.
- ▶ Three-nucleon wavefunction renormalization given by the residue of the three-nucleon propagator about the pole.
- ▶ LO three-nucleon wavefunction renormalization is

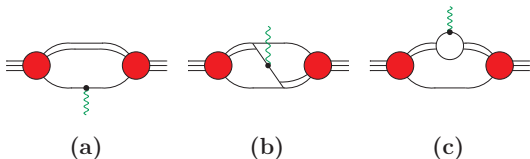
$$Z_\psi^{\text{LO}} = \frac{\pi}{\Sigma'_0(B)}.$$

- ▶ NNLO three-body force h_2 fit to triton binding energy and NNLO correction to H_0 fit to doublet S -wave nd scattering length.
- ▶ Total of **2** three-body inputs at NNLO.

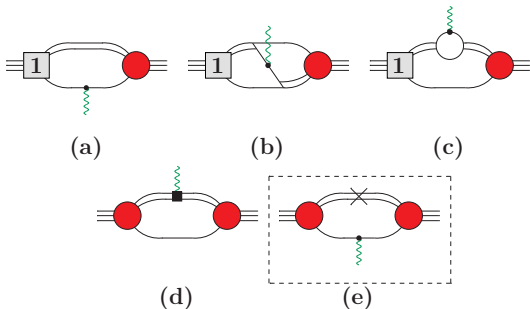


Three-Nucleon “generic” Form Factor

Three-nucleon LO “generic” form factor given by the three diagrams



NLO “generic” form factor



Form Factor Couplings

Generic form factor can be expanded as

$$F(Q^2) = a \left(1 - \frac{1}{6} \langle r^2 \rangle Q^2 + \dots \right)$$

The couplings for the form factors of interest are given by

| | Charge | Magnetic | Axial |
|--------|---|---|--|
| 1B LO | $-e\hat{N}^\dagger \hat{N} \hat{A}_0$ | $\hat{N}^\dagger (\kappa_0 + \tau_3 \kappa_1) \boldsymbol{\sigma} \cdot \mathbf{B} \hat{N}$ | $\frac{g_A}{\sqrt{2}} \hat{N}^\dagger \sigma_i \tau_+ \hat{N} \hat{A}_i^+$ |
| 2B NLO | $e c_0 t \hat{t}_i^\dagger \hat{t}_i \hat{A}_0$ | $e \frac{L_1}{2} \hat{t}^{j\dagger} \hat{s}_3 \mathbf{B}_j - e \frac{L_2}{2} i \epsilon^{ijk} \hat{t}_i^\dagger \hat{t}_j \mathbf{B}_k$ | $l_{1,A} \hat{s}_-^\dagger \hat{t}_i \hat{A}_i^-$ |
| a | Z | μ | $\langle \mathbf{G} \mathbf{T} \rangle$ |

Table: List of couplings for form factors of interest and their physical values at $Q^2 = 0$.

LO Form Factor

The LO form factor for $Q^2 = 0$ is

$$F_0(0) = 2\pi M_N \left(\tilde{\Gamma}_0(q) \right)^T \otimes \left\{ \frac{\pi}{2} \frac{\delta(q - \ell)}{q^2 \sqrt{\frac{3}{4}q^2 - M_N B}} \begin{pmatrix} c_{11} + a_{11} & c_{12} \\ c_{21} & c_{22} + a_{22} \end{pmatrix} \right.$$

$$\left. + \frac{1}{q^2 \ell^2 - (q^2 + \ell^2 - M_N B)^2} \begin{pmatrix} b_{11} - 2a_{11} & b_{12} + 3(a_{11} + a_{22}) \\ b_{21} + 3(a_{11} + a_{22}) & b_{22} - 2a_{22} \end{pmatrix} \right\} \otimes \tilde{\Gamma}_0(\ell),$$

The coefficients for various form factors are given by

| Form factor | a_{11} | a_{22} | b_{11} | b_{12} | b_{21} | b_{22} | c_{11} | c_{12} | c_{21} | c_{22} |
|--------------------------|----------------|----------------|---------------|---------------|---------------|----------------|----------|---------------|---------------|---------------|
| $F_C^{^3\text{H}}(Q^2)$ | 0 | $\frac{2}{3}$ | -1 | 1 | 1 | $\frac{1}{3}$ | 1 | 0 | 0 | $\frac{1}{3}$ |
| $F_C^{^3\text{He}}(Q^2)$ | 1 | $\frac{1}{3}$ | 0 | 2 | 2 | $-\frac{4}{3}$ | 1 | 0 | 0 | $\frac{5}{3}$ |
| $F_W^{\text{GT}}(Q^2)$ | $-\frac{1}{3}$ | $-\frac{1}{3}$ | $\frac{5}{3}$ | $\frac{1}{3}$ | $\frac{1}{3}$ | $\frac{5}{3}$ | 0 | $\frac{2}{3}$ | $\frac{2}{3}$ | 0 |
| $F_W^{\text{F}}(Q^2)$ | 1 | $-\frac{1}{3}$ | 1 | 1 | 1 | $-\frac{5}{3}$ | 0 | 0 | 0 | $\frac{4}{3}$ |

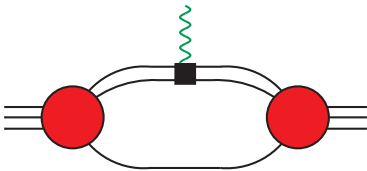
Table: Values of coefficients for the LO ${}^3\text{H}$ and ${}^3\text{He}$ axial and charge form factors.

NLO Form Factor

NLO correction to “generic” form factor at $Q^2 = 0$

$$\begin{aligned} F_1(0) &= 2\pi M_N \left(\tilde{\Gamma}_1(q) \right)^T \otimes \left\{ \frac{\pi}{2} \frac{\delta(q - \ell)}{q^2 \sqrt{\frac{3}{4}q^2 - M_N B_0}} \begin{pmatrix} c_{11} + a_{11} & c_{12} \\ c_{21} & c_{22} + a_{22} \end{pmatrix} \right. \\ &\quad \left. + \frac{1}{q^2 \ell^2 - (q^2 + \ell^2 - M_N B_0)^2} \begin{pmatrix} b_{11} - 2a_{11} & b_{12} + 3(a_{11} + a_{22}) \\ b_{21} + 3(a_{11} + a_{22}) & b_{22} - 2a_{22} \end{pmatrix} \right\} \otimes \tilde{\Gamma}_0(\ell) \\ &\quad + 2\pi M_N \left(\tilde{\Gamma}_0(q) \right)^T \otimes \left\{ \frac{\pi}{2} \frac{\delta(q - \ell)}{q^2 \sqrt{\frac{3}{4}q^2 - M_N B_0}} \begin{pmatrix} c_{11} + a_{11} & c_{12} \\ c_{21} & c_{22} + a_{22} \end{pmatrix} \right. \\ &\quad \left. + \frac{1}{q^2 \ell^2 - (q^2 + \ell^2 - M_N B_0)^2} \begin{pmatrix} b_{11} - 2a_{11} & b_{12} + 3(a_{11} + a_{22}) \\ b_{21} + 3(a_{11} + a_{22}) & b_{22} - 2a_{22} \end{pmatrix} \right\} \otimes \tilde{\Gamma}_1(\ell) \\ &\quad - 4\pi M_N \left(\tilde{\Gamma}_0(q) \right)^T \otimes \left\{ \frac{\pi}{2} \frac{\delta(q - \ell)}{q^2} \begin{pmatrix} \frac{1}{2}\rho_t a_{11} + d_{11} & d_{12} \\ d_{21} & \frac{1}{2}\rho_s a_{22} + d_{22} \end{pmatrix} \right\} \otimes \tilde{\Gamma}_0(\ell), \end{aligned}$$

NLO Form Factor (cont.)



| Form factor | d_{11} | d_{12} | d_{21} | d_{22} |
|--------------------------|---------------------|----------------------|----------------------|--------------------------------|
| $F_C^{^3\text{H}}(Q^2)$ | $\frac{1}{2}\rho_t$ | 0 | 0 | $\frac{1}{3}\frac{1}{2}\rho_s$ |
| $F_C^{^3\text{He}}(Q^2)$ | $\frac{1}{2}\rho_t$ | 0 | 0 | $\frac{5}{3}\frac{1}{2}\rho_s$ |
| $F_M^{^3\text{H}}(Q^2)$ | $-\frac{2}{3}L_2$ | $\frac{1}{3}L_1$ | $\frac{1}{3}L_1$ | 0 |
| $F_M^{^3\text{He}}(Q^2)$ | $-\frac{2}{3}L_2$ | $-\frac{1}{3}L_1$ | $-\frac{1}{3}L_1$ | 0 |
| $F_W^{GT}(Q^2)$ | 0 | $\frac{1}{3}l_{1,A}$ | $\frac{1}{3}l_{1,A}$ | 0 |

Table: Values of coefficients for the NLO corrections to (d)-type diagrams for the ${}^3\text{H}$ and ${}^3\text{He}$ magnetic, charge, and axial form factors.

Radii

Generic form factor given by

$$F(Q^2) = a \left(1 - \frac{1}{6} \langle r^2 \rangle Q^2 + \dots \right)$$

Calculating only Q^2 contribution for diagram-(a) gives

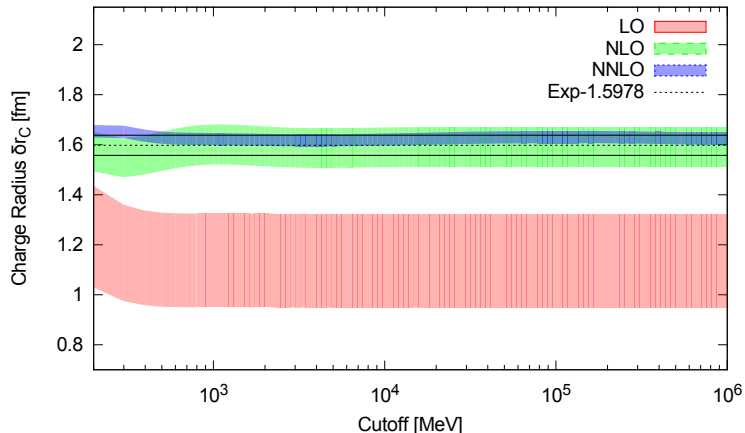
$$\begin{aligned} \frac{1}{2} \frac{\partial^2}{\partial Q^2} F_n^{(a)}(Q^2) \Big|_{Q^2=0} &= Z_\psi^{\text{LO}} \sum_{i,j=0}^{i+j \leq n} \left\{ \tilde{\mathcal{G}}_i^T(p) \otimes \mathcal{A}_{n-i-j}(p, k) \otimes \tilde{\mathcal{G}}_j(k) \right. \\ &\quad \left. + 2\tilde{\mathcal{G}}_i^T(p) \otimes \mathcal{A}_{n-i}(p) \delta_{j0} + \mathcal{A}_n \delta_{i0} \delta_{j0} \right\}, \end{aligned}$$

Triton Charge Radius

LO EFT(\not{p}) $r_C = 2.1 \pm .6$ fm (Platter and Hammer (2005)) [nucl-th/0509045](#)

NLO EFT(\not{p}) $r_C = 1.6 \pm .2$ fm (Kirscher et al. (2010)) [arXiv:0903.5538](#)

NNLO EFT(\not{p}) $r_C = 1.62 \pm .03$ fm (Vanasse (2016)) [arXiv:1512.03805](#)



The iso-scalar and iso-vector combination of magnetic moments are

$$\mu_s = \frac{1}{2} (\mu_{^3\text{He}} + \mu_{^3\text{H}}) \quad , \quad \mu_v = \frac{1}{2} (\mu_{^3\text{He}} - \mu_{^3\text{H}}) ,$$

μ_s only depends on κ_0 and L_2 , while μ_v only depends on κ_1 and L_1 at NLO.

| | μ_s | μ_v | L_1 fit |
|-----|------------|-----------|--------------------------------------|
| LO | 0.440(152) | -2.31(78) | N/A |
| NLO | 0.421(50) | -2.20(26) | σ_{np} |
| NLO | 0.421(50) | -2.56(31) | $\mu_{^3\text{H}}$ |
| NLO | 0.421(50) | -2.50(30) | σ_{np} and $\mu_{^3\text{H}}$ |
| Exp | 0.426 | -2.55 | N/A |

Table: Table of three-nucleon iso-scalar and iso-vector magnetic moments compared to experiment. The different NLO rows are different fits for L_1 and are organized the same as the previous table.

NLO two-body magnetic currents given by

$$\mathcal{L}_2^{mag} = \left(e \frac{L_1}{2} \hat{t}^{j\dagger} \hat{s}_3 \mathbf{B}_j + \text{H.c.} \right) - e \frac{L_2}{2} i \epsilon^{ijk} \hat{t}_i^\dagger \hat{t}_j \mathbf{B}_k.$$

L_2 is fit to deuteron magnetic moment and L_1 is typically fit to cold np capture cross section (σ_{np})

Magnetic moments and polarizabilities also calculated to NLO by
(Kirscher et al. (2017)) arXiv:1702.07268

| | $\mu_{^3\text{H}}$ | $\mu_{^3\text{He}}$ | $r_M^{^3\text{H}}$ fm | $r_M^{^3\text{He}}$ fm | σ_{np} mb |
|-----|--------------------|---------------------|-----------------------|------------------------|-------------------|
| LO | 2.75(95) | -1.87(73) | 1.40(24) | 1.49(26) | 325.2 ± 225.6 |
| NLO | 2.62(31) | -1.78(33) | 1.83(11) | 1.92(11) | 334.2 ± 79.7 |
| NLO | 2.98(36) | -2.14(26) | 1.77(11) | 1.83(11) | 370.47 ± 88.4 |
| NLO | 2.92(35) | -2.08(25) | 1.78(11) | 1.85(11) | 364.5 ± 87.0 |
| Exp | 2.979 | -2.127 | 1.84(18) | 1.97(15) | $334.2(5)$ |

Table: Values of magnetic moments and magnet radii for three-nucleon systems and σ_{np} to NLO compared to experiment. The first NLO row is for L_1 fit to σ_{np} , the second NLO row for L_1 fit to the ^3H magnetic moment ($\mu_{^3\text{H}}$), and the final NLO row is L_1 fit to both σ_{np} and $\mu_{^3\text{H}}$.

Bound State Observables for $3N$ Systems

(Vanasse (2016)+(2017)). arXiv:1512.03805 + arXiv:1706.02665

| Observable | LO | NLO | NNLO | Exp. |
|-------------------------------------|-----------|-----------|---------|------------|
| ^3H : r_C [fm] | 1.14(19) | 1.59(8) | 1.62(3) | 1.5978(40) |
| ^3He : r_C [fm] | 1.26(21) | 1.72(8) | 1.74(3) | 1.7753(54) |
| ^3H : r_m [fm] | 1.40(24) | 1.78(11) | – | 1.840(181) |
| ^3He : r_m [fm] | 1.49(26) | 1.85(11) | – | 1.965(153) |
| ^3H : μ_m [μ_N] | 2.75(92) | 2.92(35) | – | 2.98 |
| ^3He : μ_m [μ_N] | -1.87(73) | -2.08(25) | – | -2.13 |

Calculation of LO triton charge radius in unitary limit gives

$$mE_{3B} \langle r_c^2 \rangle = 0.224\dots$$

Using analytical techniques in

(Braaten and Hammer (2006)) cond-mat/0410417 it can be shown that $mE_{3B} \langle r_c^2 \rangle = (1 + s_0^2)/9 = 0.224\dots$ in the unitary limit.

Tritium β -decay

Half life $t_{1/2}$ of tritium given by

$$\frac{(1 + \delta_R)f_V}{K/G_V^2} t_{1/2} = \frac{1}{\langle \mathbf{F} \rangle^2 + f_A/f_V g_A^2 \langle \mathbf{GT} \rangle^2}$$

The Gamow-Teller matrix element is

$$\frac{\langle \mathbf{GT} \rangle_{\text{Exp}}}{\sqrt{3}} = 0.9551 \quad , \quad \frac{\langle \mathbf{GT} \rangle_0}{\sqrt{3}} = 0.9807 \quad , \quad \frac{\langle \mathbf{GT} \rangle_{0+1}}{\sqrt{3}} = 0.9935$$

Fitting L_{1A} to the GT-matrix element gives

$$L_{1A} = 3.46 \pm 1.19 \text{ fm}^3$$

Compares well to lattice prediction

$$L_{1A} = 3.9(0.1)(1.0)(0.3)(0.9) \text{ fm}^3$$

Gamow-Teller and Wigner-symmetry

The GT-matrix element is given by

$$\langle \mathbf{GT} \rangle \simeq \sqrt{3}(P_S + P_D/3 - P_{S'}/3)$$

In Wigner-SU(4) limit $P_{S'} = 0$ and $P_S = 1$ hence $\langle \mathbf{GT} \rangle = \sqrt{3}$ and can also be seen by

$$\begin{aligned}\langle \mathbf{GT} \rangle &= \langle {}^3\text{He} \| \sum_i \sigma^{(i)} \tau_+^{(i)} \| {}^3\text{H} \rangle \\ &= \langle {}^3\text{He} \| \sum_i \sigma^{(i)} \| {}^3\text{He} \rangle \\ &= \langle {}^3\text{He} \| \boldsymbol{\sigma} \| {}^3\text{He} \rangle \\ &= \sqrt{3}\end{aligned}$$

Fermi matrix element

Half life $t_{1/2}$ of tritium given by

$$\frac{(1 + \delta_R)f_V}{K/G_V^2} t_{1/2} = \frac{1}{\langle \mathbf{F} \rangle^2 + f_A/f_V g_A^2 \langle \mathbf{GT} \rangle^2}$$

In the isospin limit the Fermi matrix element reduces to

$$\begin{aligned}\langle \mathbf{F} \rangle &= \left\langle {}^3\text{He} \right\| \sum_i \tau_+^{(i)} \left\| {}^3\text{H} \right\rangle \\ &= \left\langle {}^3\text{He} \right\| \mathbf{1} \left\| {}^3\text{He} \right\rangle \\ &= 1\end{aligned}$$

Indeed, we find $\langle \mathbf{F} \rangle = 1$.

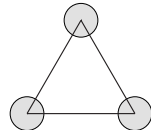
Consequences of Wigner-symmetry and Unitarity

Wigner-limit: $a_0 = a_1$ and $r_0 = r_1$

Unitary limit: $a_0 = a_1 = \infty$

Wigner-breaking $\mathcal{O}(\delta)$: $\delta = \frac{1/a_1 - 1/a_0}{1/a_1 + 1/a_0}$

Wigner-breaking all orders:



| | Unitary | Wigner | $\mathcal{O}(\delta)$ | δ all orders |
|--------------------|---------|--------|-----------------------|---------------------|
| LO EFT($\not p$) | 1.10 | 1.22 | 1.08/1.19 | 1.14/1.26 |
| $\mathcal{O}(r)$ | 1.42 | 1.66 | 1.58/1.70 | 1.59/1.72 |
| Experiment | | | | 1.5978(40)/1.775(5) |

Table: $^3\text{H}/^3\text{He}$ charge radius in unitary and Wigner-limit ([Vanassee and Phillips \(2016\)](#)) arXiv:1607.08585

In Wigner-limit it can be shown both analytically and numerically

$$\mu_{(^3\text{H})} = \mu_p = 2.79 \frac{e}{2M_N} \quad , \quad \mu_{(^3\text{He})} = \mu_n = -1.91 \frac{e}{2M_N}$$

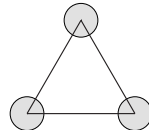
Consequences of Wigner-symmetry and Unitarity

Wigner-limit: $a_0 = a_1$ and $r_0 = r_1$

Unitary limit: $a_0 = a_1 = \infty$

Wigner-breaking $\mathcal{O}(\delta)$: $\delta = \frac{1/a_1 - 1/a_0}{1/a_1 + 1/a_0}$

Wigner-breaking all orders:



| | Unitary | Wigner | $\mathcal{O}(\delta)$ | δ all orders |
|--------------------|---------|--------|-----------------------|---------------------|
| LO EFT($\not p$) | 1.10 | 1.22 | 1.08/1.19 | 1.14/1.26 |
| $\mathcal{O}(r)$ | 1.42 | 1.66 | 1.58/1.70 | 1.59/1.72 |
| Experiment | | | | 1.5978(40)/1.775(5) |

Table: $^3\text{H}/^3\text{He}$ charge radius in unitary and Wigner-limit ([Vanassee and Phillips \(2016\)](#)) arXiv:1607.08585

In Wigner-limit it can be shown both analytically and numerically

$$\mu_{(^3\text{H})} = \mu_p = 2.79 \frac{e}{2M_N} \quad , \quad \mu_{(^3\text{He})} = \mu_n = -1.91 \frac{e}{2M_N}$$

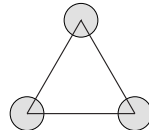
Consequences of Wigner-symmetry and Unitarity

Wigner-limit: $a_0 = a_1$ and $r_0 = r_1$

Unitary limit: $a_0 = a_1 = \infty$

Wigner-breaking $\mathcal{O}(\delta)$: $\delta = \frac{1/a_1 - 1/a_0}{1/a_1 + 1/a_0}$

Wigner-breaking all orders:



| | Unitary | Wigner | $\mathcal{O}(\delta)$ | δ all orders |
|--------------------|---------|--------|-----------------------|---------------------|
| LO EFT($\not p$) | 1.10 | 1.22 | 1.08/1.19 | 1.14/1.26 |
| $\mathcal{O}(r)$ | 1.42 | 1.66 | 1.58/1.70 | 1.59/1.72 |
| Experiment | | | | 1.5978(40)/1.775(5) |

Table: $^3\text{H}/^3\text{He}$ charge radius in unitary and Wigner-limit ([Vanassee and Phillips \(2016\)](#)) arXiv:1607.08585

In Wigner-limit it can be shown both analytically and numerically

$$\mu_{(^3\text{H})} = \mu_p = 2.79 \frac{e}{2M_N} \quad , \quad \mu_{(^3\text{He})} = \mu_n = -1.91 \frac{e}{2M_N}$$

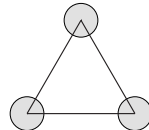
Consequences of Wigner-symmetry and Unitarity

Wigner-limit: $a_0 = a_1$ and $r_0 = r_1$

Unitary limit: $a_0 = a_1 = \infty$

Wigner-breaking $\mathcal{O}(\delta)$: $\delta = \frac{1/a_1 - 1/a_0}{1/a_1 + 1/a_0}$

Wigner-breaking all orders:



| | Unitary | Wigner | $\mathcal{O}(\delta)$ | δ all orders |
|--------------------|---------|--------|-----------------------|---------------------|
| LO EFT($\not p$) | 1.10 | 1.22 | 1.08/1.19 | 1.14/1.26 |
| $\mathcal{O}(r)$ | 1.42 | 1.66 | 1.58/1.70 | 1.59/1.72 |
| Experiment | | | | 1.5978(40)/1.775(5) |

Table: $^3\text{H}/^3\text{He}$ charge radius in unitary and Wigner-limit ([Vanassee and Phillips \(2016\)](#)) arXiv:1607.08585

In Wigner-limit it can be shown both analytically and numerically

$$\mu_{(^3\text{H})} = \mu_p = 2.79 \frac{e}{2M_N} \quad , \quad \mu_{(^3\text{He})} = \mu_n = -1.91 \frac{e}{2M_N}$$

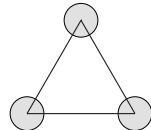
Consequences of Wigner-symmetry and Unitarity

Wigner-limit: $a_0 = a_1$ and $r_0 = r_1$

Unitary limit: $a_0 = a_1 = \infty$

Wigner-breaking $\mathcal{O}(\delta)$: $\delta = \frac{1/a_1 - 1/a_0}{1/a_1 + 1/a_0}$

Wigner-breaking all orders:



| | Unitary | Wigner | $\mathcal{O}(\delta)$ | δ all orders |
|--------------------|---------|--------|-----------------------|---------------------|
| LO EFT($\not p$) | 1.10 | 1.22 | 1.08/1.19 | 1.14/1.26 |
| $\mathcal{O}(r)$ | 1.42 | 1.66 | 1.58/1.70 | 1.59/1.72 |
| Experiment | | | | 1.5978(40)/1.775(5) |

Table: $^3\text{H}/^3\text{He}$ charge radius in unitary and Wigner-limit ([Vanassee and Phillips \(2016\)](#)) arXiv:1607.08585

In Wigner-limit it can be shown both analytically and numerically

$$\mu_{(^3\text{H})} = \mu_p = 2.79 \frac{e}{2M_N} \quad , \quad \mu_{(^3\text{He})} = \mu_n = -1.91 \frac{e}{2M_N}$$

Conclusions and Future directions

- ▶ Charge radii of ^3H and ^3He reproduced well at NNLO in EFT($\not{\pi}$).
- ▶ Magnetic moments and radii reproduced within errors at NLO in EFT($\not{\pi}$).
- ▶ L_{1A} prediction agrees with LQCD prediction. Better prediction for L_{1A} will further constrain EFT($\not{\pi}$) prediction for pp fusion.
- ▶ Wigner-symmetry gives good expansion for charge radii and is interesting limit for three-nucleon magnetic moments and GT-matrix element. Results should be used as benchmark.
- ▶ Reproduce analytical results in unitary limit for charge radii. Should be used as benchmark for all such calculations.